

Electronic Supporting Information

Repeat proteins as versatile scaffolds for arrays of redox-active Fe-S clusters

Sara H. Mejias,^{a†} Zahra Bahrami-Dizicheh,^{†b} Mantas Liutkus,^c Dayn Joshep Sommer,^b Andrei Astashkin,^d Gerdenis Kodis,^b Chad Borges,^b Giovanna Ghirlanda,^{b} and Aitziber L. Cortajarena^{a,c,e,*}*

^a IMDEA-Nanociencia and Nanobiotechnology Unit Associated to the National Center for Biotechnology (CNB-CSIC), Campus de Cantoblanco, E-28049 Madrid, Spain.

^b School of Molecular Sciences, Arizona State University Tempe, AZ 85287-1604, USA.

^c CIC biomaGUNE Paseo de Miramón 182, E-20014 Donostia-San Sebastian, Spain.

^d Department of Chemistry and Biochemistry, University of Arizona Tucson, AZ, 85271, USA.

^e Ikerbasque Foundation for Science, E-48011 Bilbao, Spain.

* Corresponding author: alcortajarena@icbiomagune.es; giovanna.ghirlanda@asu.edu

A. Materials and Methods

Protein design and purification. Mutations were introduced in CTPR1 units to generate two mutated repeats C1 (Y5C and N9C) and C2 (E2C and N6C) by quick-change site directed mutagenesis. The two mutated CTPR1 units C1 and C2 were then fused to create the CTPR2_4cys gene by sequential cloning of C1 and C2 into pPro-EXHTa vector (sequence in Fig. 1). CTPR4_8cys and CTPR8_16cys genes were generated by sequential additions of two and four copies of the CTPR2_4cys gene into pPro-EXHTa vector.

The proteins were expressed in *E. coli* C41 strain with an *N*-terminal His-tag and purified using Ni-NTA affinity chromatography based on previously published protocols for His-tagged CTPR proteins,¹ using 0.5 M UREA in the lysis buffer to improve protein solubility. The proteins were then dialyzed against PBS buffer (150 mM NaCl, 50 mM phosphate, pH 7.4). Protein concentration was determined using absorbance at 280 nm with the extinction coefficient calculated from the amino acid sequence of each protein² (32110 M⁻¹ cm⁻¹ for CTPR2_4cys, 59750 M⁻¹ cm⁻¹ for CTPR4_8cys and 115030 M⁻¹ cm⁻¹ for CTPR8_16cys). TEV protease in PBS buffer with 1 mM DTT and 0.5 mM EDTA was added to remove the His-tag in a 1:20 TEV:CTPR protein molar ratio and incubated at 4 °C overnight. His-tagged TEV protease was removed using Ni-NTA affinity chromatography, in which CTPR proteins without His-tag were collected in the flow-through, while the His-tag and the tagged TEV protease remained bound to the affinity resin. CTPR proteins were dialyzed against 100 mM Tris-HCl pH 8.5 buffer and stored at -20 °C.

Incorporation of [4Fe-4S] clusters into CTPR proteins. Iron-sulfur clusters were incorporated into the designed proteins by adapting a previously established protocol.^{3,4} All reactions were performed in an anaerobic chamber (Coy Scientific) under 95% N₂ and 5% H₂ atmosphere. To a 50 μM CTPR protein solution in 100 mM Tris-HCl, pH 8.5 was added β-mercaptoethanol to a final concentration of 0.8% (v/v) (total reaction volume of 2.5 ml), and the solution was incubated for 20 min. Freshly prepared solution of ferric chloride (FeCl₃) was then added dropwise to a final concentration of 3 mM. After additional 20 min, freshly prepared solution of sodium sulfide (Na₂S) was added to a final concentration of 3 mM. The dark brown solution was incubated overnight at room temperature and was then desalted using PD-10 column (GE Healthcare), pre-equilibrated with 100 mM Tris at pH 7.5, to remove all non-protein low molecular mass contaminants and salts. The protein-cluster fractions were then collected for further characterization.

Cluster identification and quantification. UV-vis spectra were acquired using a Perkin-Elmer Lambda-35 spectrophotometer under anaerobic conditions. The absorption spectra from 230 nm to 800 nm were acquired in a 1 cm path-length quartz cuvette using a 4 nm slit-width. The spectra of the CTPR-[4Fe-4S]²⁺ proteins were acquired directly from desalted samples. Freshly prepared sodium dithionite was added to a final concentration of 1mM to reduce the clusters.

To assess the cluster incorporation quantitatively, iron and protein concentrations were measured separately in each sample. Iron concentration was determined using the ferrozine assay,⁵ and protein concentration was quantified using Bradford assay^{6,7} for CTPR2-[4Fe-4S], CTPR4-2[4Fe-4S] and CTPR8-4[4Fe-4S] proteins. The proteins were denatured at 95 °C for 15 min prior to the Bradford assay

to ensure that the Bradford reagent interacts effectively with the proteins. The relative iron/protein concentrations were then calculated.

Circular dichroism (CD) spectroscopy. CD characterization of apo proteins and of CTPR2-[4Fe-4S], CTPR4-2[4Fe-4S] and CTPR8-4[4Fe-4S] constructs in 10 mM Tris-HCl buffer pH 7.5 was performed with a JASCO J-815 spectropolarimeter, using a quartz cuvette with a path length of 0.1 cm. CD spectra were recorded from 260 to 190 nm in 1 nm increments. Thermal denaturation curves were monitored by following the CD signal at 222 nm as a function of temperature from 10 °C to 95 °C. The measurements were taken in an airtight cuvette to exclude air during the course of the experiment. CD spectra of apo proteins were recorded in the presence of excess tris(2-carboxyethyl)phosphine (TCEP) to maintain the cysteine side chains in a reduced state. Molar residue ellipticity (MRE) was calculated using cuvette path length in centimeters, and the number of amino acids of 73, 141 and 277 for CTPR2, CTPR4 and CTPR8, respectively.

Electron paramagnetic resonance (EPR) spectroscopy. Protein-cluster fractions eluted from PD-10 column were concentrated using ultrafiltration centrifugal tubes (GE Healthcare) with a molecular weight cut-off (MWCO) of 3000 Da to approximately 1 mM. The samples were reduced with 100 mM sodium dithionite in 1 M glycine buffer at pH 10.0 to a final concentration of 20 mM sodium dithionite. 10% (v/v) glycerol was then added as cryoprotectant and the samples were flash-frozen in quartz EPR tubes in liquid N₂. EPR experiments were carried out at the EPR facility of the University of Arizona, on an X-band EPR spectrometer Elexsys E500 (Bruker) equipped with a standard TE₁₀₂ resonator and an ESR900 flow cryostat (Oxford Instruments). The measurements were performed at 15 K with microwave (mw) frequency 9.335 GHz, mw power 2 mW and magnetic field modulation amplitude 0.5 mT. The numerical simulations of the EPR spectra were performed using the SimBud software available at <https://cbc.arizona.edu/research/support-services/facilities/electron-paramagnetic-resonance-epr-facility/software>. For the simulated spectra of CTPR2-[4Fe-4S], CTPR4-2[4Fe-4S] and CTPR8-4[4Fe-4S], the principal g-values (g_1, g_2, g_3) = (1.878, 1.927, 2.060), (1.878, 1.927, 2.06), (1.883, 1.927, 2.057) and the corresponding intrinsic linewidths of (8, 5, 4.5), (8, 5.5, 5) and (8, 4.7, 4.5) mT were used.

Square wave voltammetry (SWV). Electrochemical experiments were performed on a CH Instruments 1242B potentiostat in an oxygen-free glovebox using a three-electrode configuration: a glassy carbon (3 mm diameter 0.28 cm² surface area) working electrode, a platinum mesh counter electrode and a Saturated Calomel Electrode (SCE) reference electrode. Working electrode was cleaned by sequential polishing with 1 μm, 0.05 μm, and 0.03 μm alumina. Square wave voltammetry measurements were taken using 10 μM of the proteins in 100 mM Tris, 100 mM NaCl pH 7.5 electrolyte with the increment potential of 0.004 V and square wave frequency of 20 Hz. The collected data is shown without further processing.

Transient absorption spectroscopy. Transient absorption spectra and kinetics were obtained using HELIOS Fire spectrometer (Ultrafast Systems). Excitation at 400 nm was from an optical parametric amplifier (Spectra Physics) pumped with laser pulses of 100 fs at 800 nm generated by an amplified, mode-locked titanium sapphire laser system (Millennia/Tsunami/Spitfire, Spectra Physics) operating at

1kHz repetition rate. The angle between the polarization of the excitation and probe pulses was set at 54.7° (magic angle) with respect to each other to eliminate anisotropic effects associated with rotational dynamics. The instrument response function (IRF) was *ca.* 200 fs. The protein samples dissolved in 100 mM Tris pH 7.5 were loaded into a 5 mm path length tightly capped quartz cuvette (Spectrocell Inc.) inside a glovebox under nitrogen atmosphere. Solutions were stirred during the measurement using a Teflon coated stir bar to avoid excessive exposure of samples to multiple laser shots.

Data analysis. Data analysis was carried out using locally written software (ASUFIT) within a MATLAB environment (Mathworks Inc.). Decay-associated spectra were obtained by fitting the transient absorption change curves over a selected wavelength region simultaneously as described by the equation below (parallel kinetic model),

$$\Delta A(\lambda, t) = \sum_{i=1}^n A_i(\lambda) \exp(-t/\tau_i)$$

where $\Delta A(\lambda, t)$ is the observed absorption change at a given wavelength at time delay t and n is the number of kinetic components used in the fitting. A plot of $A_i(\lambda)$ versus wavelength is called a decay-associated spectrum (DAS), and represents the amplitude spectrum of the i^{th} kinetic component, which has a lifetime of τ_i . Kinetics at early decay times (<500 fs) were obscured by the strong CPM artifacts and stimulated Raman signal of water therefore it was difficult to extract useful information about the shortest-lived species, if any, from the data.

Evolution-associated difference spectra (EADS) were obtained by global analysis of the transient absorption data using a kinetic model consisting of sequentially interconverting species, e.g. 1→2→3→... n . The arrows indicate successive mono-exponential decays with increasing time constants, which can be regarded as the lifetimes of each species. Associated with each species is a lifetime and a difference spectrum. Each EADS corresponds in general to a mixture of states and does not portray the spectrum of a pure state or species. This procedure facilitates a better visualization of the evolution of transient states in the system. The global analysis procedures described here were adapted from literature methods.⁸ Random errors associated with the reported lifetimes obtained from transient absorption measurements were typically $\leq 5\%$.

References.

- 1 T. Kajander, A. L. Cortajarena and L. Regan, *Methods Mol. Biol.*, 2006, **340**, 151–170.
- 2 C. N. Pace, F. Vajdos, L. Fee, G. Grimsley and T. Gray, *Protein Sci.*, 1995, **4**, 2411–2423.
- 3 M. L. Antonkine, M. S. Koay, B. Epel, C. Breitenstein, O. Gopta, W. Gärtner, E. Bill and W. Lubitz, *Biochim. Biophys. Acta - Bioenerg.*, 2009, **1787**, 995–1008.
- 4 A. Roy, I. Sarrou, M. D. Vaughn, A. V Astashkin and G. Ghirlanda, *Biochemistry*, 2013, **52**, 7586–7594.
- 5 P. Carter, *Anal. Biochem.*, 1971, **40**, 450–458.
- 6 M. M. Bradford, *Anal. Biochem.*, 1976, **72**, 248–254.
- 7 J. J. Sedmak and S. E. Grossberg, *Anal. Biochem.*, 1977, **79**, 544–552.
- 8 I. H. M. Van Stokkum, D. S. Larsen and R. Van Grondelle, *Biochim. Biophys. Acta - Bioenerg.*, 2004, **1657**, 82–104.

B. Supporting Images and Tables

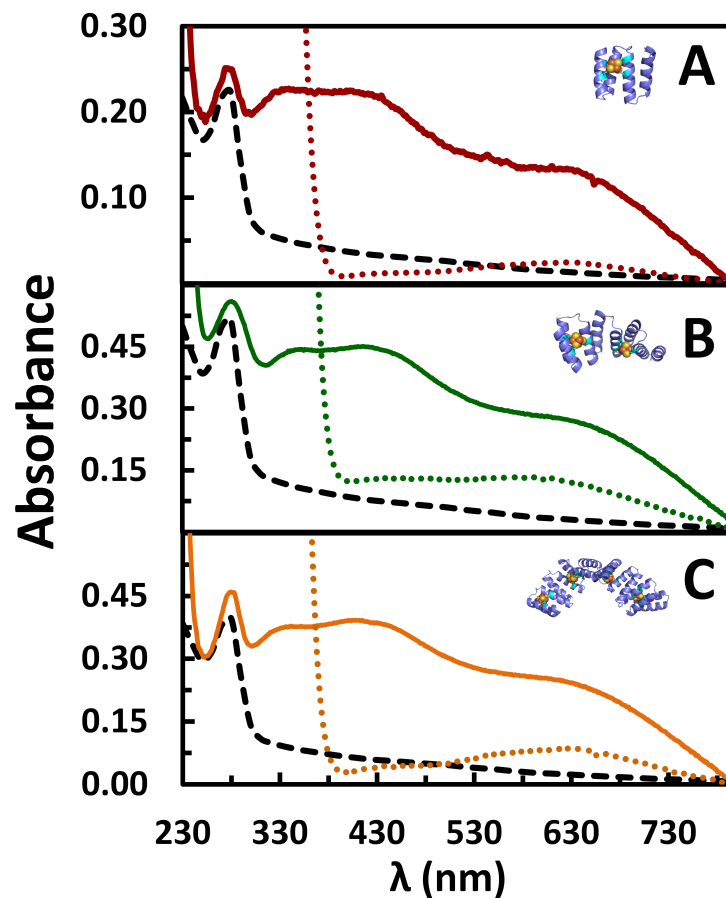


Figure S1. UV-vis characterization of CTPR-[4Fe-4S] complexes. UV-vis spectra of (A) CTPR2-[4Fe-4S], (B) CTPR4-2[4Fe-4S] and (C) CTPR8-4[4Fe-4S]. Solid red, green or orange lines: protein-cluster constructs; dotted red, green or orange lines: dithionite-reduced protein-cluster constructs; dashed black lines: apo-proteins.

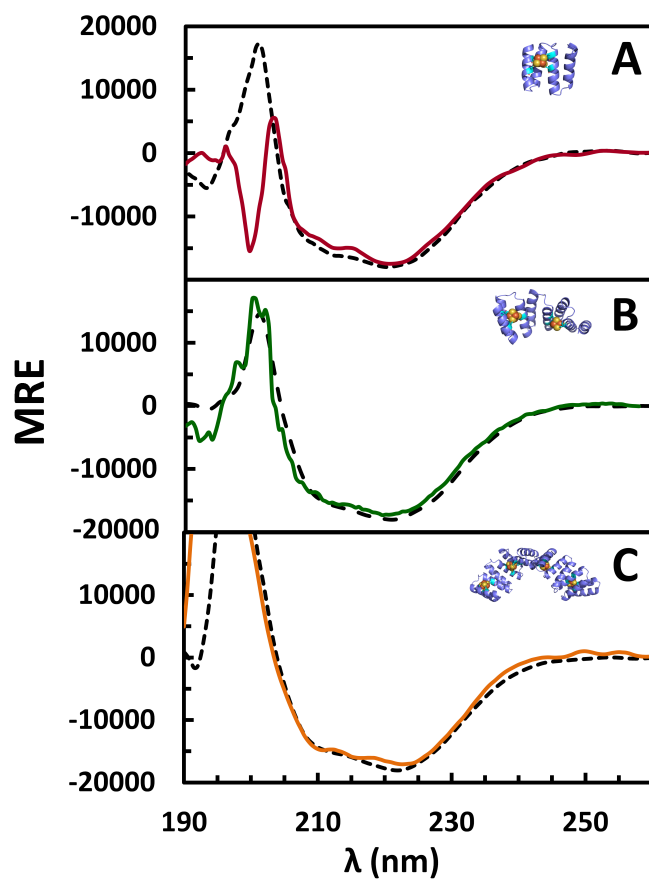


Figure S2. CD characterization of CTPR-[4Fe-4S]. CD spectra of (A) CTPR2-[4Fe-4S], (B) CTPR4-2[4Fe-4S] and (C) CTPR8-4[4Fe-4S] constructs in red, green and orange solid lines, respectively, and the corresponding apo-proteins in black dashed lines.

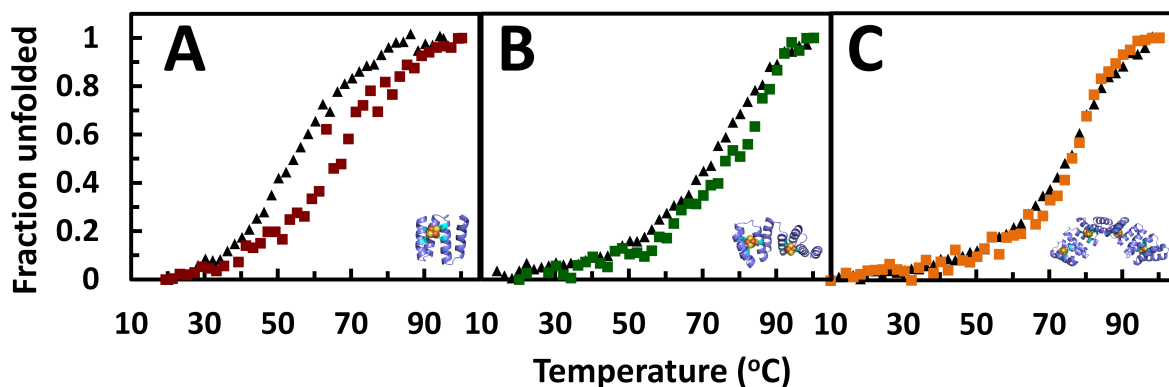


Figure S3. Thermal stability of CTPR-[4Fe-4S] complexes. Thermal denaturation of (A) CTPR2-[4Fe-4S], (B) CTPR4-2[4Fe-4S] and (C) CTPR8-4[4Fe-4S] in red, green and orange squares, respectively, and of the corresponding apo proteins (black triangles). CD signal was measured at 222 nm while the temperature was increased.

Table S1. Redox properties of the CTPR-[4Fe-4S] conjugates. Cathodic wave value (E_{pc}), anodic wave value (E_{pa}), and half wave potential ($E_{1/2}$) in volts (V) vs Standard Calomel Electrode (SCE).

	E_{pc} (V)	E_{pa} (V)	$E_{1/2}$ (V)
CTPR2-[4Fe-4S]	-0.32	-0.09	-0.21
CTPR4-2[4Fe-4S]	-0.34	-0.14	-0.24
CTPR8-4[4Fe-4S]	-0.35	-0.13	-0.24

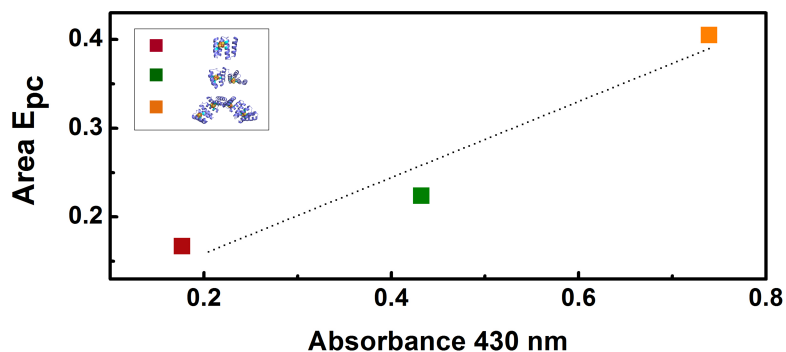


Figure S4. Dependence of redox current on [4Fe-4S] cluster population. The area of the E_{pc} peak from the square wave voltammogram (Figure 3) against sample absorbance at 430 nm. CTPR2-[4Fe-4S] in red, CTPR4-2[4Fe-4S] in green and CTPR8-4[4Fe-4S] in orange. As absorbance at 430 nm depends on cluster concentration, the trend implies a linear relationship between redox current and cluster population.

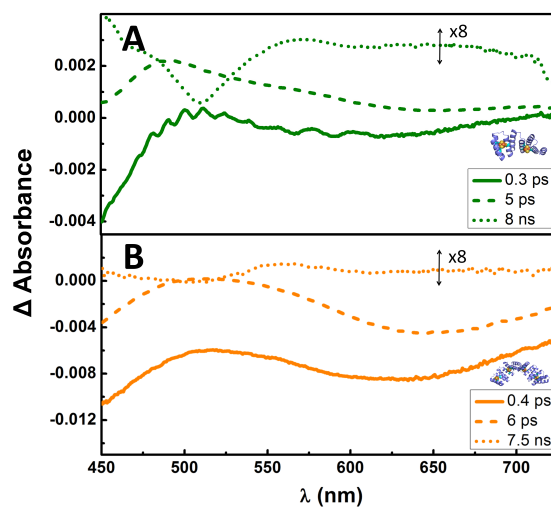


Figure S5. EADS spectra. From top to bottom, EADS of (A) CTPR4-2[4Fe-4S] and (B) CTPR8-4[4Fe-4S] obtained from global analysis of the TA data with excitation at 400 nm. Decay lifetimes are shown in the insets. Dotted lines (7.5 ns) EADS are multiplied by a factor of 8 to enhance visibility.

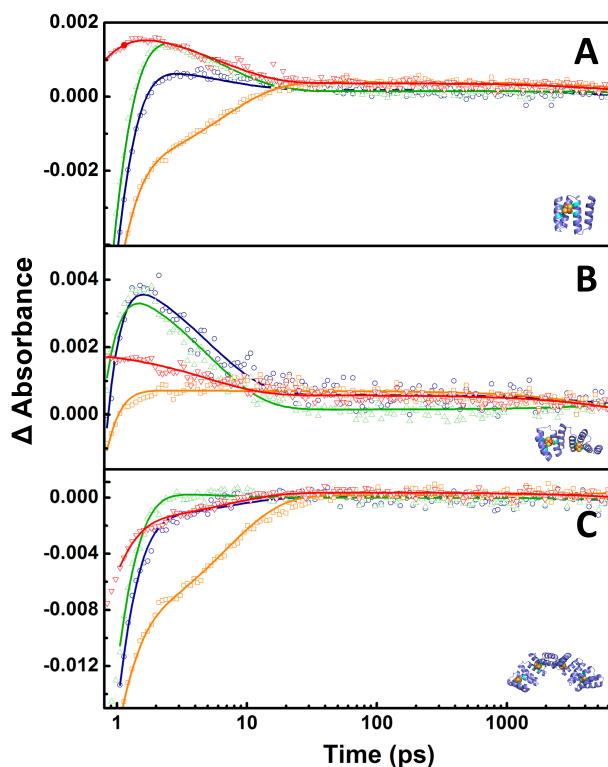


Figure S6. Transient absorption kinetics. From top to bottom, transient absorption (TA) kinetics of CTPR2-[4Fe-4S], CTPR4-2[4Fe-4S] and CTPR8-4[4Fe-4S] at different wavelengths after excitation at 400 nm. Blue for 480 nm, green for 510 nm, orange for 630 nm and red for 750 nm.